

# Monte Carlo study of the CO-poisoning dynamics in a model for the catalytic oxidation of CO

Ezequiel V. Albano<sup>a)</sup> and Joaquín Marro

*Instituto Carlos I de Física Teórica y Computacional, Facultad de Ciencias, Universidad de Granada, E-18071, Granada, Spain*

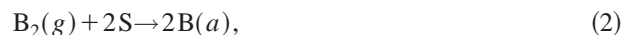
(Received 4 April 2000; accepted 15 September 2000)

The poisoning dynamics of the Ziff–Gulari–Barshad [Phys. Rev. Lett. **56**, 2553 (1986)] model, for a monomer–dimer reaction, is studied by means of Monte Carlo simulations. Studies are performed within the monomer absorbing state and close to the coexistence point. Analysis of the average poisoning time ( $\tau_p$ ) allows us to propose a phenomenological scaling approach in which  $\tau_p$  diverges logarithmically with the lattice side and algebraically with the distance to the coexistence point. The structure of monomer clusters during poisoning is analyzed and compared with observations at coexistence. © 2000 American Institute of Physics. [S0021-9606(00)51346-4]

## I. INTRODUCTION

The study of far-from-equilibrium many particle systems is a topic of current interest in many branches of physics, chemistry, biology, geology, sociology, and even economics.<sup>1–3</sup> Unlike the case of equilibrium statistical physics, nonequilibrium situations lack a well established general framework. Therefore, recent progress in this field has mainly been obtained by studying specific models by means of computer simulations, mean-field approaches, field theoretical calculations, phenomenological scaling, etc.<sup>4</sup>

Among the broad scope of nonequilibrium phenomena, a rather modest branch, namely, the study of surface chemical reactions, has recently attracted growing attention.<sup>5,6</sup> In fact, lattice gas models have been extensively used to explain a wide range of experimental observations in catalysis.<sup>7–10</sup> Various lattice models, including dimer–dimer, dimer–monomer, monomer–monomer, and its variations, which aim to simulate catalyzed reactions such as the oxidation of hydrogen, the oxidation of carbon monoxide, the reaction  $\text{NO} + \text{CO}$ , the  $\text{NH}_3$  synthesis, etc.,<sup>5,6</sup> have already been studied. Within this context the Ziff–Gulari–Barshad (ZGB) model<sup>11</sup> has become the archetype for the study of nonequilibrium critical phenomena in surface reaction processes. The ZGB model, aimed to mimic the reaction between  $\text{CO} \equiv \text{A}$  and  $\text{O}_2 \equiv \text{B}_2$  on a Pt-surface, assumes a simplified three-step Langmuir–Hinshelwood process,<sup>11</sup> namely,



where S is an empty site on the surface, while (a) and (g) refer to the adsorbed and gas phases, respectively.

The ZGB model uses a square lattice to represent the catalytic surface, and it can be simulated, using the Monte Carlo method, as follows: (i) A or B<sub>2</sub> molecules are selected randomly with relative probabilities  $Y_A$  and  $Y_B$ , respectively. These probabilities are the relative impingement rates of both species, which are proportional to their partial pressures. Due to the normalization,  $Y_A + Y_B = 1$ , the model has a single parameter, i.e.,  $Y_A$ . If the selected species is A, a surface site is selected at random and, if that site is vacant, A is adsorbed on it [Eq. (1)]. Otherwise, if that site is occupied, the trial ends and a new molecule is selected. If the selected species is (B<sub>2</sub>), a pair of nearest neighbor sites is selected at random and the molecule is adsorbed on them only if they are both vacant [Eq. (2)]. (ii) After each adsorption event, the nearest neighbors of the added molecule are examined in order to account for the reaction in Eq. (3). If more than one [B(a),A(a)] nearest-neighbor pair is identified, one is selected at random and removed from the surface (for more details on the ZGB model and the simulation technique see, e.g., Refs. 4,5,11).

The interest in the ZGB model arises due to its varied and complex nonequilibrium behavior. In two dimensions the system reaches asymptotically ( $t \rightarrow \infty$ ), a stationary state whose nature depends solely on the parameter  $Y_A$ . For  $Y_A \leq Y_{1A} \cong 0.387\ 368$  ( $Y_A \geq Y_{2A} \cong 0.525\ 540$ ) the surface becomes irreversibly ‘‘poisoned’’ by B(A) species, while a steady state with sustained production of AB is observed for  $Y_{1A} < Y_A < Y_{2A}$ . At  $Y_{1A}$  and  $Y_{2A}$  the ZGB model exhibits irreversible phase transitions (IPT’s) between the reactive regime and poisoned states, that are of second and first order, respectively. The second-order IPT, which belongs to the universality class of directed percolation, is very well understood.<sup>12,13</sup> Regrettably, the lack of experimental evidence on such kind of IPT makes the topic of academic interest mostly. In contrast, there are clear evidences of a first-order transition in the catalytic oxidation of CO on Pt(111).<sup>7–9,14</sup> However, this transition is so far not well understood.<sup>15</sup>

The aim of this work is to study the dynamics of

<sup>a)</sup>Permanent address: Instituto de Investigaciones Físicoquímicas Teóricas y Aplicadas, (INIFTA), CONICET, UNLP, CIC (Bs. As.), Sucursal 4, Casilla de Correo 16, (1900) La Plata, Argentina. Fax: 0054-221-4254642; electronic mail: ealbano@inifta.unlp.edu.ar

A-poisoning close to the first-order IPT of the ZGB model. For this purpose, we have performed extensive Monte Carlo simulations. The analysis of which have motivated us to propose a phenomenological scaling law for the average poisoning time ( $\tau_p$ ) as a function of the sample size and the distance to the coexistence point  $Y_{2A}$ . The scaling behavior of  $\tau_p$  for a much simpler reaction, namely, the monomer-monomer lattice gas model, has recently been studied in detail,<sup>16–18</sup> which allows us to establish useful comparisons.

The manuscript is organized as follows: in Sec. II the simulation method and main definitions are formulated. Some selected results are presented and discussed in Sec. III, and our conclusions are stated in Sec. IV.

## II. BRIEF DESCRIPTION OF THE MONTE CARLO SIMULATION METHOD

The ZGB model is simulated on the square lattice of side  $L$ , assuming periodic boundary conditions and using standard techniques.<sup>4,5,11</sup> The time unit is the Monte Carlo step (mcs) in which each site of the sample is visited once, on the average. Simulations are performed on lattices of side  $128 \leq L \leq 2048$ ; and averages are taking over  $10^5$ – $10^3$  different samples, depending on the side.

Runs are always performed starting from empty lattices for values of the parameter within the absorbing state but close to coexistence, i.e.,  $Y_A > Y_{2A}$ . Each run stops when the sample becomes trapped in the absorbing state, that is, a fully A-covered sample is obtained. During this poisoning process the average coverage with A-species ( $\theta_A$ ) is recorded from time to time. The distribution of poisoning times,  $D(t)$ , which gives the probability of the sample to become poisoned at time  $t$ , is also measured. The first moment of the distribution, namely, the average poisoning time,  $\tau_p$ , is also evaluated.

## III. RESULTS AND DISCUSSION

Figure 1 provides some qualitative insight on the dynamics of the A-poisoning process. This shows plots of  $\theta_A$  vs  $t$  as obtained during the poisoning process for different values of  $Y_A$ . As expected, curves saturate faster for larger  $Y_A$ -values (i.e., far from coexistence). In these cases one has an almost linear growth of  $\theta_A$  at early times followed by an abrupt saturation. However, closer to coexistence, (see for instance, the data for  $Y_A=0.53$ ), one can observe a slow increase of the coverage at early times, followed by a faster (linear) one within an intermediate time regime. Subsequently, saturation is also observed. This behavior can be understood with the aid of the snapshot configurations in Fig. 2. Figure 2(a), obtained for  $t=100$  mcs with a coverage  $\theta_A=0.098$  illustrate the initial nucleation of many small A-islands. These islands are unstable, as one may conclude by continuously monitoring the system evolution along the interval  $10 \text{ mcs} < t < 100$  mcs. Subsequently, for  $t=500$  mcs and  $\theta_A=0.286$ , as in Fig. 2(b), one has that a few clusters have grown beyond a certain critical size thus becoming essentially stable. As suggested by the graphs in Fig. 1, these stable clusters then become in contact with each other [see, for instance, Fig. 2(c), for  $t=750$  mcs and  $\theta_A=0.449$ ], finally producing a massive

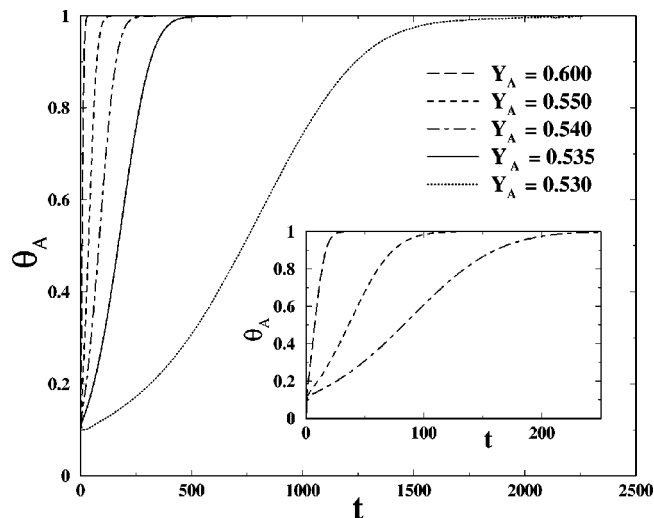


FIG. 1. Plot of the time evolution of the A-coverage obtained for different values of  $Y_A$  as indicated in the figure. Results averaged over 1000 different samples using lattices of side  $L=256$ . The inset shows a zoom of the data corresponding to the largest  $Y_A$ -values.

A-cluster, as illustrated in Fig. 2(d) for  $t=1000$  mcs and  $\theta_A=0.728$ . At longer times, the single A-cluster prevails surrounding small islands of active sites.

It should be noted that, due to the lack of energetic interactions between A-species in the ZGB model, one should expect the operation of rather weak (or vanishing small) ‘‘effective surface tension’’ effects. In fact, recent simulation studies on the behavior of A-rich interfaces close to coexistence<sup>19–21</sup> have shown that the dynamic of the propagation of the interface can be described in terms of the Kardar–Parisi–Zhang (KPZ) equation,<sup>22</sup>

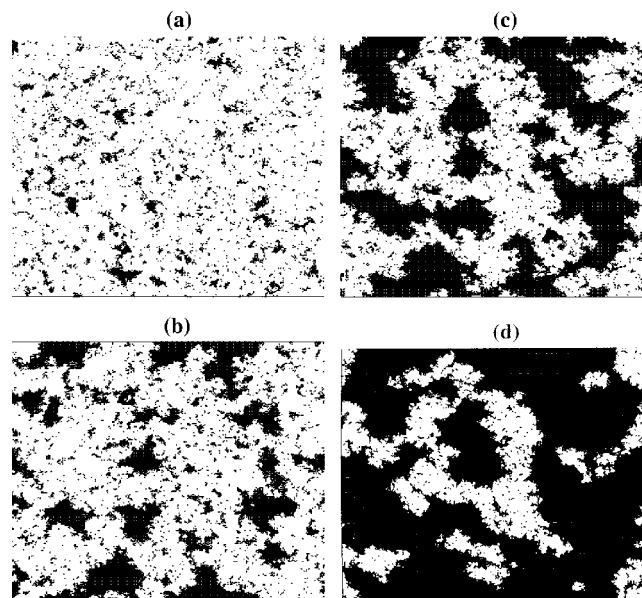


FIG. 2. Snapshot configurations obtained during the A-poisoning process assuming  $Y_A=0.53$  and for lattices of side  $L=256$ . A-species are shown as black points while B-species and empty sites are left in white. (a)  $t=100$  mcs,  $\theta_A=0.098$ ; (b)  $t=500$  mcs,  $\theta_A=0.286$ ; (c)  $t=750$  mcs and  $\theta_A=0.449$ ; and (d)  $t=1000$  mcs and  $\theta_A=0.728$ .

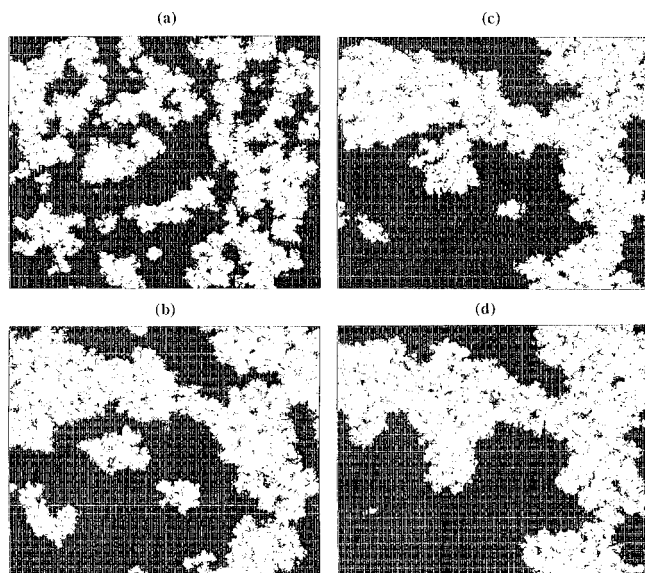


FIG. 3. Snapshot configurations obtained, at different times, after switching abruptly the system from a stationary regime of the standard ensemble (with  $P_A=0.51$ ) to the constant-coverage ensemble with  $\theta_A=0.500$ . The lattice is of side  $L=256$ . Same symbols as in Fig. 2. (a)  $t=100$  mcs, (b)  $t=500$  mcs, (c)  $t=750$  mcs, and (d)  $t=1000$  mcs. More details in the text.

$$\dot{h} = D\nabla^2 h + (\lambda/2)(\nabla h)^2 + \eta(\mathbf{r}, t), \quad (4)$$

where  $h(\mathbf{r}, t)$  is the height of the interface at location  $\mathbf{r}$  and time  $t$ . The first term of the right-hand side of Eq. (4) describes the relaxation of the interface by a surface tension  $D$ , while the second term is the lowest-order nonlinear term that can appear in the interface-growth equation, and accounts for the dependence of the grow rate on the local slope of the interface. In most theoretical studies the stochastic term  $\eta(\mathbf{r}, t)$  is assumed to be Gaussian and  $\delta$ -function correlated. It should be noted that the first term of Eq. (4) with  $D > 0$  is necessary in order to stabilize the interface propagation. Thus,  $D$  is naturally identified as the ‘‘effective kinetic surface tension.’’<sup>19</sup>

So, we expect that such a weak ‘‘effective surface tension’’ causes small clusters to be of rather irregular shape with pronounced convexity [Fig. 2(b)]. This property of clusters, is in marked contrast with other systems where the surface tension arises due to energetic interactions, as, e.g., the droplets of the Ising model upon spinodal decomposition.<sup>23</sup> Also, large A-clusters exhibit a quite dense bulk with a vanishingly small number of holes [see, e.g., Fig. 2(c)] and, therefore, they look so far much different from those of standard percolation where the hole-size distribution extends over a wide scale close to criticality and shows scale invariance just at the critical point.<sup>24</sup>

It is also interesting to compare the structure of A-clusters formed during the poisoning process with those obtained at coexistence using the constant-coverage ensemble method<sup>25</sup> which allows one to obtain metastable configurations. Figure 3 is a set of snapshot configurations obtained, at different times, after switching abruptly the system from a stationary regime of the standard ensemble (with  $P_A=0.51$ ) to the constant-coverage ensemble with  $\theta_A=0.500$ . The latter corresponds to coexistence and the snap-

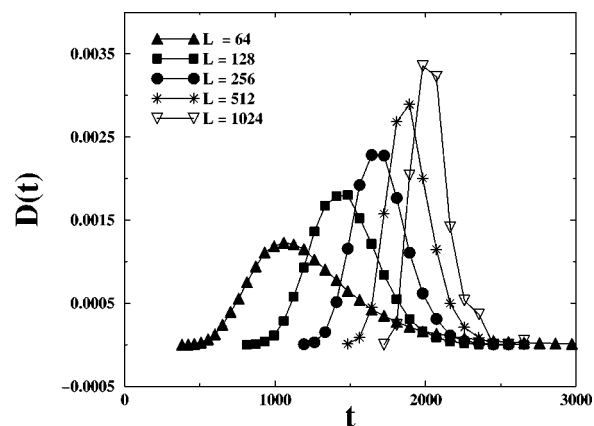


FIG. 4. Plot of distribution of poisoning times  $D(t)$  for  $Y_A=0.530$  and different values of the lattice side as indicated.

shots are obtained for the same times as in Fig. 2 in order to allow for a comparison. Already for  $t=100$  mcs compact clusters of A-species have been developed. However, these clusters include holes of active sites covering a large range of length scales. Subsequently, for  $t \geq 500$  mcs a single (large) cluster of A-species becomes essentially stable, while only few small islands are present. Notice that, as time increases, the holes of active sites steadily shrink and tend to disappear, e.g., for  $t=1000$  mcs in Fig. 3(d). At this stage, the coexistence of two phases, namely, an A-rich phase characterized by a large A-cluster, and a reactive state with small A-clusters, can clearly be distinguished. Here the growth of the massive A-cluster (stable phase) is due to the displacement of an unstable phase (the reactive regime). This picture is quite different from that inferred from the poisoning process, as one easily concludes after comparison of Figs. 2 and 3.

The quantitative behavior of our data, also allows us some conclusions concerning (phenomenological) scaling approach for the poisoning process. Figure 4 shows the distribution of poisoning times,  $D(t)$  vs  $t$ , close to coexistence for lattices of different side. The Gaussian shape of the left-hand side of the distributions turns into a long-tailed shape at larger times, reflecting a nonvanishing number of events with long-lived reactive configurations. It is also clear that increasing the lattice side,  $\tau_p$  increases and the distributions become sharper.

The dependence of  $\tau_p$  on both  $L$  and  $Y_A$  is illustrated in Fig. 5(a). Our best fit for the lattice-side dependence, obtained keeping  $Y_A$  constant, suggest a logarithmic behavior, i.e.,

$$\tau_p \propto \ln(L^2), \quad (5)$$

which is indicated in Fig. 5(b). It is likely that a slight departure from Eq. (5) that we observe for the largest lattice used ( $L=2048$ ) very close to coexistence ( $Y_A=0.53$ ) may be due to stochastic fluctuations and the lack of appropriated statistics. It is also interesting to compare the behavior of the ZGB model with that of a much simpler system, e.g., the monomer–monomer (MM) model. In fact, the MM,  $A(a) + B(a) \rightarrow AB(g) + 2S$ , has been solved exactly<sup>16,17</sup> and the

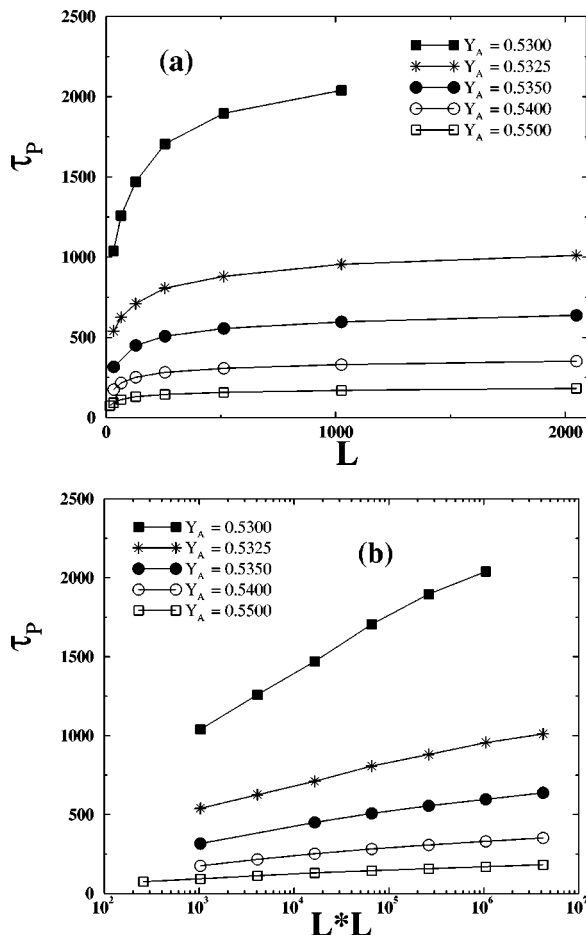


FIG. 5. (a) Plot of  $\tau_p$  vs  $L$  and (b) lineal-logarithmic plot of  $\tau_p$  vs  $L^2$ . Results obtained for different values of  $Y_A$  as indicated.

saturation time just at the phase transition has been shown to have, except for logarithmic corrections, a linear dependence on the number of catalytic sites, namely,

$$\tau_p \propto L^2(1 + C \ln(L)). \quad (6)$$

Monte Carlo simulations agree with this (exact) prediction and suggest  $C \approx 0.16$ .<sup>18</sup> Equation (6) can be interpreted on simple grounds. In the MM model, each reaction event removes exactly one A and one B, so that the difference between A- and B-species adsorbed on the surface at any time equals the difference in the number of A- and B-species that have struck free sites of the surface. Poisoning occurs when such number equals the number of sites on the surface,  $L^2$ , and this occurs after a number of successful adsorption events of the order of  $L^4$ , since the fluctuations grow as the square root of the number of trials. Since a Monte Carlo time step involves  $L^2$  trials,  $\tau_p$  is expected to grow proportionally to  $L^2$ . As time goes on, unsuccessful adsorption events, which must also be considered in the measurement of the time, prevail due to the high density of occupied sites. Consequently the growth of  $\tau_p$  becomes somewhat slower, which leads to the logarithmic correction.<sup>18</sup> Because of the fact that the poisoning time of the MM model was studied at the critical point and our study of the ZGB model was performed just above coexistence, poisoning in the ZGB model is a much faster process than in the case of the MM model. We

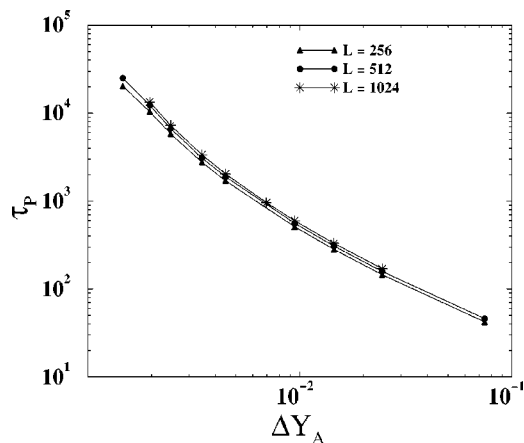


FIG. 6. Log-log plot of  $\tau_p$  vs the distance to the coexistence point obtained for different values of the lattice side as indicated.

expect that this behavior would also hold at coexistence of the ZGB model. We argue that this may be due to the intrinsic asymmetry in the adsorption rules of dimers and monomers, respectively. In fact, at coexistence and close above it, the double site requirements for dimer adsorption clearly favors A-poisoning. For example, let us consider empty sites on the bulk of A-clusters. A single site can only be occupied by A-species. Two nearest-neighbor sites can be poisoned with A-species with a probability ( $\approx 88\%$ ) larger than that for  $B_2$ -adsorption. Three adsorption sites can be blocked by A-adsorption on the central one with probability  $\approx 0.5$  and subsequently A-poisoning must occur. Also, for these reasons, A-clusters are compact with a vanishing small number of holes (see, e.g., the snapshots of Fig. 2). Similarly, the propagation and growth of the interface of A-clusters due to A-adsorption at perimeter sites may be slightly favored provided that such interface is rough enough, as, e.g., it can be observed in the snapshots of Fig. 2. This effect is caused by the larger relative abundance of single vs double sites at rough interfaces which arises due to the blocking effect of already adsorbed A-species.

While Eq. (6) can be understood on the basis of simple phenomenological arguments (as discussed above, see also Ref. 18), we can only give some hints in order to explain our findings of Eq. (5). Beyond coexistence the interface of the A-rich phase is unstable and moves with constant velocity.<sup>19,20</sup> So, if the behavior would be dominated by a single A-cluster one would expect the poisoning time to grow linearly with  $L$ . A different scenario would be the simultaneous growth of a uniform density of clusters, which would lead to a poisoning time essentially independent of  $L$ . Obviously, these are not quite the cases. However, the logarithmic term may be due to a weak correction to the prediction of the latter scenario when the competitive growth of many clusters with interfacial fluctuations is considered.

On the other hand, Fig. 6 shows plots of  $\tau_p$  vs  $\Delta = Y_A - Y_{2A}$  obtained using lattices of different side. These plots have a clear curvature, which is consistent with an algebraic dependence such as

$$\tau_p \propto \Delta^\alpha, \quad (7)$$

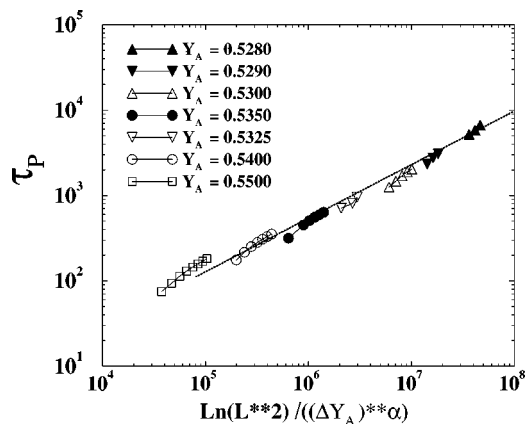


FIG. 7. Scaled plot of the data shown in Figs. 5 and 6 according to Eq. (8). A straight line, biased by the data points corresponding to larger lattices, has been drawn in order to guide the eyes.

in the limit  $\Delta \rightarrow 0$ , where we obtain  $\alpha \approx 2.7$ .

Combining Eqs. (5) and (7) we come to suggest a phenomenological scaling relation of the form

$$\tau_p \propto \ln(L^2) \Delta^\alpha, \quad L \rightarrow \infty, \quad \Delta \rightarrow 0. \quad (8)$$

The validity of this behavior is demonstrated in Fig. 7 which shows an acceptable data collapse. It should be noted that the velocity of propagation of the interface of the A-clusters ( $V_p$ ) close to coexistence behaves as  $V_p \propto \Delta^{-\gamma}$  with  $\gamma \approx 1$ .<sup>19,20</sup> So, the logarithmic term in Eq. (8) prevents us from establishing a relationship between the exponents  $\alpha$  and  $\gamma$ .

#### IV. CONCLUSION

The dynamics of A-poisoning close to the coexistence point has been studied for the ZGB model. It is shown that A-poisoning proceeds through the nucleation and growth of many clusters with a vanishing small surface tension. Therefore, both the structure and the growth mechanism of A-clusters during the poisoning process substantially differ from that observed at phase coexistence. Based on Monte Carlo results, we propose a phenomenological scaling rela-

tion for the poisoning process in the ZGB model close to coexistence, showing that the average time for poisoning is proportional to  $\ln(L^2)$ . That is, this process is expected to be much faster in the ZGB model than in the monomer-monomer model.

#### ACKNOWLEDGMENTS

This work is supported financially by CONICET, UNLP, CIC (As. As.), ANPCyT (Argentina), and the Volkswagen Foundation (Germany) and DGEIC (Spain) Project No. PB97-0842.

- <sup>1</sup>G. Nicolis and I. Prigogine, *Self-Organization in Nonequilibrium Systems* (Wiley-Interscience, New York, 1977).
- <sup>2</sup>H. Haken, *Synergetics* (Springer-Verlag, New York, 1983).
- <sup>3</sup>See, e.g., a set of very interesting articles recently published in *Science* **284**, 79 (1999).
- <sup>4</sup>J. Marro and R. Dickman, *Nonequilibrium Phase Transitions in Lattice Models* (Cambridge University Press, Cambridge, U.K., 1999).
- <sup>5</sup>E. V. Albano, *Chem. Rev.* **3**, 389 (1996).
- <sup>6</sup>E. V. Albano, in *Surface Chemical Reactions*, edited by M. Borowko (Marcel Dekker, New York, 2000) (in press).
- <sup>7</sup>K. Christmann, *Introduction to Surface Physical Chemistry* (Steinkopff Verlag, Darmstadt, 1991), pp. 1–274.
- <sup>8</sup>J. H. Block, M. Ehsasi, and V. Gorodetskii, *Prog. Surf. Sci.* **42**, 143 (1993).
- <sup>9</sup>M. Ehsasi *et al.*, *J. Chem. Phys.* **91**, 4949 (1989).
- <sup>10</sup>R. Imbhil and G. Ertl, *Chem. Rev.* **95**, 697 (1995).
- <sup>11</sup>R. M. Ziff, E. Gulari, and Y. Barshad, *Phys. Rev. Lett.* **56**, 2553 (1986).
- <sup>12</sup>G. Grinstein, Z.-W. Lai, and D. A. Browne, *Phys. Rev. A* **40**, 4820 (1989).
- <sup>13</sup>I. Jensen, H. C. Fogedby, and R. Dickman, *Phys. Rev. A* **41**, 3411 (1990).
- <sup>14</sup>M. Berdau *et al.*, *J. Chem. Phys.* **110**, 11551 (1999).
- <sup>15</sup>R. A. Monetti, A. Rozenfeld, and E. V. Albano, *cond-mat/9911040*, 1999.
- <sup>16</sup>P. L. Krapivsky, *Phys. Rev. A* **45**, 1067 (1992).
- <sup>17</sup>E. Clément, P. Leroux-Hugon, and L. M. Sander, *Phys. Rev. Lett.* **67**, 1661 (1991).
- <sup>18</sup>C. A. Voigt and R. M. Ziff, *J. Chem. Phys.* **107**, 7397 (1997).
- <sup>19</sup>J. W. Evans and T. R. Ray, *Phys. Rev. E* **50**, 4302 (1994).
- <sup>20</sup>R. H. Goodman, D. S. Graff, L. M. Sander, P. Leroux-Hugon, and E. Clément, *Phys. Rev. E* **52**, 5904 (1995).
- <sup>21</sup>E. V. Albano, *Phys. Rev. E* **55**, 7144 (1997).
- <sup>22</sup>M. Kardar, G. Parisi, and Y. C. Zhang, *Phys. Rev. Lett.* **56**, 889 (1986).
- <sup>23</sup>K. Binder, M. H. Kalos, J. L. Lebowitz, and J. Marro, *Adv. Colloid Interface Sci.* **10**, 173 (1979).
- <sup>24</sup>D. Stauffer and A. Aharony, *Introduction to the Percolation Theory*, 2nd. ed. (Taylor and Francis, London 1992).
- <sup>25</sup>R. M. Ziff and B. J. Brosilow, *Phys. Rev. A* **46**, 4630 (1992).